



## Molecular Crystals and Liquid Crystals Science and Technology. Section A. Molecular Crystals and Liquid Crystals

Publication details, including instructions for authors and subscription information:  
<http://www.tandfonline.com/loi/gmcl19>

### Unified Surface Anchoring Energy for Cyano-and Fluorinated Nematic Liquid Crystals on a Polymer Alignment Layer

Shoichi Ishihara<sup>a</sup>, Makoto Tsuji<sup>b</sup> & Akihiko Sugimura<sup>b</sup>

<sup>a</sup> LCD Development Group, Display Device Development Center, Matsushita Electric Industrial Co., Ltd., 3-1-1, Yagumo-Nakamachi, Moriguchi, Osaka, 570-8501, Japan

<sup>b</sup> Department of Information Systems Engineering, Osaka Sangyo University, 3-1-1, Nakagaito, Daito-shi, Osaka, 574-8530, Japan

Version of record first published: 24 Sep 2006

To cite this article: Shoichi Ishihara, Makoto Tsuji & Akihiko Sugimura (1999): Unified Surface Anchoring Energy for Cyano-and Fluorinated Nematic Liquid Crystals on a Polymer Alignment Layer, *Molecular Crystals and Liquid Crystals Science and Technology. Section A. Molecular Crystals and Liquid Crystals*, 329:1, 161-170

To link to this article: <http://dx.doi.org/10.1080/10587259908025937>

PLEASE SCROLL DOWN FOR ARTICLE

Full terms and conditions of use: <http://www.tandfonline.com/page/terms-and-conditions>

This article may be used for research, teaching, and private study purposes. Any substantial or systematic reproduction, redistribution, reselling, loan, sub-licensing, systematic supply, or distribution in any form to anyone is expressly forbidden.

The publisher does not give any warranty express or implied or make any representation that the contents will be complete or accurate or up to date. The accuracy of any instructions, formulae, and drug doses should be independently verified with primary sources. The publisher shall not be liable for any loss, actions, claims, proceedings, demand, or costs or damages whatsoever or howsoever caused arising directly or indirectly in connection with or arising out of the use of this material.

## Unified Surface Anchoring Energy for Cyano- and Fluorinated Nematic Liquid Crystals on a Polymer Alignment Layer

SHOICHI ISHIHARA<sup>a</sup>, MAKOTO TSUJI<sup>b</sup> and AKIHIKO SUGIMURA<sup>b</sup>

<sup>a</sup>LCD Development Group, Display Device Development Center, Matsushita Electric Industrial Co., Ltd., 3-1-1, Yagumo-Nakamachi, Moriguchi, Osaka 570-8501, Japan and <sup>b</sup>Department of Information Systems Engineering, Osaka Sangyo University, 3-1-1, Nakagaito, Daito-shi, Osaka 574-8530, Japan

The unified surface anchoring energy, which has been proposed to describe the generalized anisotropic interaction between the nematic director and the substrate, was investigated for nematic slabs of various cyano- and fluorinated liquid crystals (LCs) on a polyimide alignment layer. A saturation voltage method, combined with a conventional optical method, was employed for determining the unified surface anchoring energy. The surface anchoring strength (SAS) was found to vary over the range  $10^{-4}$  to  $10^{-3}$  [J/m<sup>2</sup>] depending on the LC molecular structure. It was also found that the values of SAS change with respect to the tilt angle in opposite directions for the cyano- and fluorinated LCs.

**Keywords:** liquid crystal; continuum theory; molecular structure; surface anchoring energy

### INTRODUCTION

There is considerable interest in the director distribution in the bulk and at the surfaces of a nematic liquid crystal (LC) slab, in both basic science and technology<sup>[1]</sup>. It is well-known that the director distribution in the bulk of a LC slab is affected by the substrate surface, as well as by externally applied fields, such as the electric and magnetic fields. That is, the surface anchoring strength (SAS) determines the director profile in a LC cell with applied fields. Hence it is one of the major factors which influence

the LCD performance.

The investigation and clarification of the surface anchoring mechanism leads to the enhancement of display performance such as an enlargement of a viewing angle, the solution of image-sticking problem which has been seen in the in-plane switching mode cells and, moreover, the invention of a new LCD mode.

To describe the interaction between LC molecules and alignment film surface, Rapini and Papoular (RP) have introduced a simple phenomenological expression for the interfacial surface anchoring energy per unit area which describes the anisotropic interaction between the nematic director and the substrate<sup>[3]</sup>. In the RP model the anchoring energy reflects the ability of the director to deviate from the easy direction<sup>[2]</sup>. On the basis of the RP model and its modifications, there are many reports in the literature on the measurement of anchoring energies<sup>[1,4]</sup>.

Recently, on the basis of a general RP model, a unified surface anchoring energy has been proposed with which to predict the director deformation of a twisted chiral nematic sample theoretically<sup>[5-6]</sup>. In this model the surface anchoring energy is generalized to describe an interfacial energy, in which the surface anchoring energy is not separated into polar and azimuthal surface anchoring energies, independent of each other, as is often used. The unified surface anchoring model has been used to measure the anchoring strength,  $A$ , for the nematic phase of 4-pentyl-4'-cyanobiphenyl (5CB) and polyimide Langmuir-Blodgett substrates with ultra thin film thickness  $< 10\text{nm}$ <sup>[7]</sup>. The model has also led to the proposal of a saturation voltage method<sup>[8]</sup> as a simple measurement method of SAS.

In this study, we have measured SAS of cyano- and fluorinated LCs on a polyimide interface by using a saturation voltage method based on a unified surface anchoring theory, and have investigated the relation between the LC molecular structures, SAS and the tilt angle.

## EXPERIMENTAL

### Materials

Cyano-LCs (Sample No. :CN1-CN5) and fluorinated LCs (Sample No. :F1-F7) were used in the SAS measurement. Table 1 and Table 2 show the composition and physical properties of these LCs, respectively. The number inside parentheses following abbreviations of LC molecular structures in Table 1 shows the blending ratio of each component. The molecular structures of the LCs and their abbreviations are shown in Table 3.

TABLE 1 Compositions of liquid crystal mixtures used

Cell No.	Abbreviation of LC Components (wt.%) <sup>†</sup>
CN1	3PCH(30), 5PCH(40), 7PCH(30)
CN2	3PCH(25), 5PCH(35), 7PCH(25), 5BCH(15)
CN3	3PDX(25), 4PDX(50), 5PDX(25)
CN4	5CB(50), 7CB(50)
CN5	5CB(100)
F1	2HPFF, 3HPFF, 5HPFF (equivalent weight mixture)
F2	2H2PFF(40), 3H2PFF(20), 5H2PFF(40)
F3	5HEF(37.5), 7HEF(37.5), 3IHEF(12.5), 5HHEF(12.5)
F4	7PFF(40), 2HPFF(20), 3HPFF(20), 5HPFF(20)
F5	3PyFF(30), 5PyFF(30), 4PyBF(20), 5PyBF(20)
F6	5PF(17), 6PF(14), 7PF(13), 3TF(15), 5TF(18), 7TF(23)
F7	2HBFF(25), 3HBFF(25), 5HBFF(50)

<sup>†</sup>The first figure of each abbreviation denotes a number of an alkyl chain.

TABLE 2 Physical characteristics of liquid crystal mixtures used

Cell No.	T <sub>c</sub> (°C)	$\epsilon_{  }$	$\Delta\epsilon$	k <sub>11</sub> (pN)	k <sub>22</sub> (pN)	k <sub>33</sub> (pN)	n <sub>e</sub>	n <sub>o</sub>	$\Delta n$
CN1	52.3	15.1	10.2	7.83	8.59	16.24	1.606	1.488	0.118
CN2	72.4	14.9	10.4	9.65	7.93	22.04	1.628	1.491	0.137
CN3	40.5	23.5	13.6	5.05	3.73	7.93	1.588	1.488	0.100
CN4	38.8	16.3	10.5	6.90	5.73	10.19	1.709	1.527	0.182
CN5	35.3	17.0	11.0	6.37	3.81	8.60	1.707	1.530	0.177
F1	112.5	8.5	4.8	10.28	10.63	24.22	1.562	1.483	0.079
F2	95.3	7.9	4.3	9.42	10.76	27.00	1.553	1.480	0.073
F3	60.5	6.2	2.1	7.47	5.65	11.88	1.537	1.473	0.064
F4	40.8	8.0	3.7	4.38	5.28	8.65	1.535	1.480	0.055
F5	31.7	17.5	10.6	5.01	5.20	6.26	1.667	1.530	0.137
F6	27.0	7.4	3.6	5.59	3.04	6.11	1.647	1.512	0.135
F7	93.1	9.4	5.5	10.03	7.05	14.68	1.649	1.507	0.142

### Cell Preparation

The pairs of substrates were assembled with rubbing direction anti-parallel. Polyimide(PI) (SE-7492, Nissan Chemical Industries, Ltd.) was used as an alignment film. The PI films were deposited on the substrates from dilute polymer solutions by a spinning method and then baked at 180°C for an hour. The thickness of PI films was measured by the alphastep<sup>R</sup> (TENCOR

INSTRUMENT') and found to be about 80nm. The area of the electrode was 2cm<sup>2</sup> and the spacing  $\ell$  for LC cells was set at 6.5 $\mu$ m by using plastic beads. The spacing was measured by the LCD thickness meter TM-230N(Canon Sales Co., Inc.).

After filling with the LC, all LC cells were annealed at a temperature higher than the nematic-isotropic transition temperature (clearing temperature: T<sub>c</sub>) by 20 degrees for an hour.

TABLE 3 Molecular structures of liquid crystals

PCH	$R-\text{H}-\text{C}_6\text{H}_4-\text{CN}$
BCH	$R-\text{H}-\text{C}_6\text{H}_4-\text{C}_6\text{H}_4-\text{CN}$
PDX	$R-\text{C}_6\text{H}_4-\text{CN}$
CB	$R-\text{C}_6\text{H}_4-\text{C}_6\text{H}_4-\text{CN}-\text{F}$
HBFF	$R-\text{H}-\text{C}_6\text{H}_4-\text{C}_6\text{H}_4-\text{F}-\text{F}$
HPFF	$R-\text{H}-\text{C}_6\text{H}_4-\text{C}_6\text{H}_4-\text{F}-\text{F}$
H2PFF	$R-\text{H}-\text{CH}_2\text{CH}_2-\text{C}_6\text{H}_4-\text{F}-\text{F}$
HEF	$R-\text{H}-\text{COO}-\text{C}_6\text{H}_4-\text{F}$
HHEF	$R-\text{H}-\text{C}_6\text{H}_4-\text{COO}-\text{C}_6\text{H}_4-\text{F}$
PF	$R-\text{H}-\text{C}_6\text{H}_4-\text{F}-\text{F}$
PFF	$R-\text{H}-\text{C}_6\text{H}_4-\text{F}-\text{F}$
PyBF	$R-\text{C}_6\text{H}_4-\text{C}_6\text{H}_4-\text{F}-\text{F}$
PyFF	$R-\text{C}_6\text{H}_4-\text{C}_6\text{H}_4-\text{F}-\text{F}$
TF	$R-\text{C}_6\text{H}_4-\text{C}\equiv\text{C}-\text{C}_6\text{H}_4-\text{F}$

#### Pretilt Angle Measurement

The pretilt angle, which is the tilt angle of the easy axis in LC cells, was measured by the Optical Measuring System OMS-P3(Chuo Precision Industrial Co., Ltd.) at 25°C.

#### Surface Anchoring Strength Measurement (Saturation Voltage Method)

The saturation voltage method derived from the unified surface anchoring model has already been reported as a simple measurement method of SAS<sup>[8]</sup>. Assuming that the easy directions and SASs at the top and bottom substrates surfaces are the same, the following relationship between

the surface anchoring strength  $A$  and the saturation voltage  $U_s$  for a nematic LC slab with a homogeneous director orientation was derived:

$$A = \frac{U_s k_{22} \sqrt{\epsilon_0 \Delta \epsilon k_{33}}}{\ell k_{11}} \tanh \left( \frac{U_s}{2} \sqrt{\frac{\epsilon_0 \Delta \epsilon}{k_{33}}} \right). \quad (1)$$

where,  $k_{11}$ ,  $k_{22}$ , and  $k_{33}$  are the splay, twist, and bend elastic constants of the LC, respectively,  $\Delta \epsilon$  is the dielectric anisotropy,  $\epsilon_0$  is dielectric constant in the space, and  $\ell$  is the film thickness.

Moreover, in the case of practical LCs, the formula  $U_s > 2\sqrt{k_{33}/(\epsilon_0 \Delta \epsilon)}$  is satisfied. And so, Eq.(1) is simplified as follows;

$$A = \frac{U_s k_{22} \sqrt{\epsilon_0 \Delta \epsilon k_{33}}}{\ell k_{11}}. \quad (2)$$

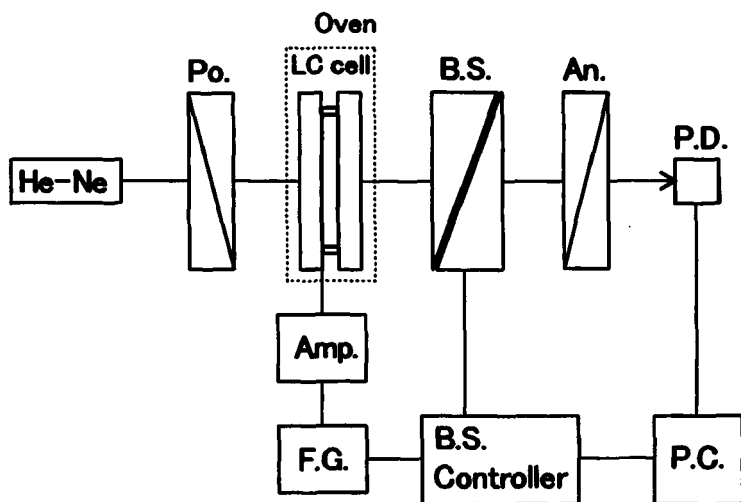


FIGURE 1 Experimental setup to measure the optical retardation of a LC slab

The experimental setup used to measure  $U_s$  is shown schematically in Figure 1. Po. An. P.D. and P.C. are the polarizer, analyzer, the photo-detector and the personal computer, respectively. BS is a Babinet-Soleil compensator to measure the optical retardation from the sample. The output of

a He-Ne laser (Spectra Physics Co., model-117A) is linearly polarized by means of a polarizer (Polaroid HN-38). The laser beam is passed through the thermostated LC slab with its axis at an angle of 45 degrees with respect to the polarization direction of the beam. The resulting elliptically polarized light passes through a BS compensator (Siguma Koki Co., Auto Babinet Soleil Stage B-83). Its optical retardation is adjusted by means of an electrical stepper motor to compensate for the optical phase difference due to the birefringence of the LC slab which depends on the slab thickness, the refractive indices of the LC and an applied external voltage supplied through a function generator F.G (Hewlett Packard Co., HP-8116A). The precision in the optical retardation for  $\lambda = 632.8\text{nm}$  is  $1.66 \times 10^{-5} \mu\text{m/step}$ . By this precise compensation the light transmitted through the analyzer which is crossed with the polarizer has a minimum beam intensity.

The saturation voltage  $U_s$  is obtained by plotting the measured optical retardation  $((\Delta n \ell))$  of the LC cell against the reciprocal of the applied voltage<sup>[9]</sup>. The value of  $U_s$  is given by the extrapolated value of  $1/U$  when  $\Delta n \ell$  is zero.

RESULTS AND DISCUSSION

The values of SAS measured with a PI alignment layer for the various LCs plotted as a function of the reduced temperature  $(T(K)/T_c(K))$  are given in Figures 2 and 3 for the cyano- and fluorinated LCs respectively. The values of SAS for the various LCs at  $T/T_c=0.95$  were determined from Figures 2 and 3 and are given in Table 4.

TABLE 4 Numerical data of surface anchoring strength at  $T/T_c=0.95$

Cell No.	$A \times 10^4 \text{ [J/m}^2\text{]}$	Cell No.	$A \times 10^4 \text{ [J/m}^2\text{]}$
CN1	11.2	F1	2.83
CN2	3.90	F2	5.82
CN3	1.72	F3	1.07
CN4	2.75	F4	2.52
CN5	3.45	F5	2.55
		F6	2.20
		F7	4.07



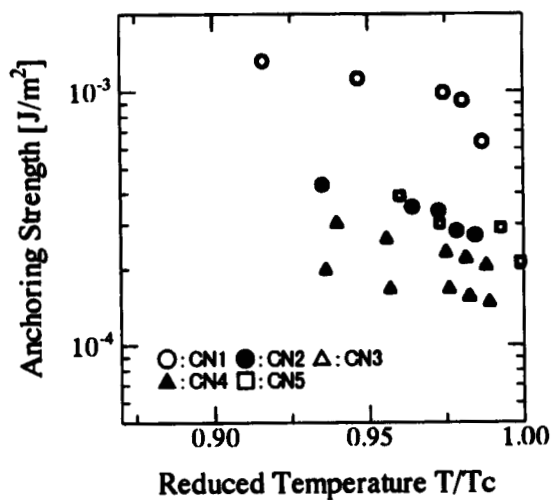


FIGURE 2 The dependence of the unified anchoring strength on the reduced temperature for the cyano-liquid crystals

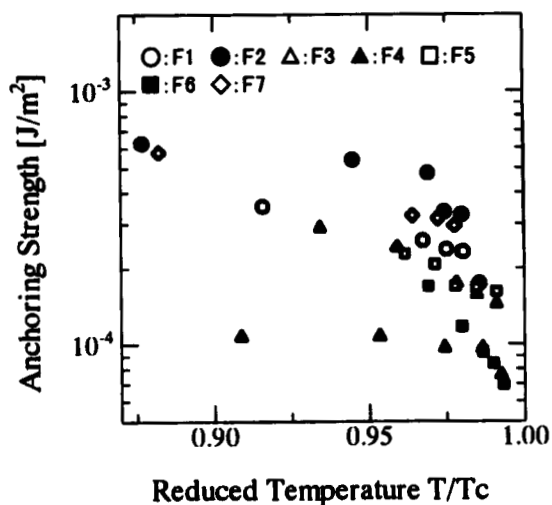


FIGURE 3 The dependence of the unified anchoring strength on the reduced temperature for the fluorinated liquid crystals

From the values in Table 4, the trends regarding the relationship between the molecular structure of LCs and their SAS values may be summarised as follows:

1. The introduction of an ethylene linkage in LCs containing two terminal fluorines leads to an increase in SAS (compare F1 and F2).
2. Oxygen containing LCs appear to have the smallest values of SAS (F3 and CN3).
3. The larger the electronic density in the molecular skeleton of the LC, the smaller the SAS, as can be seen in the series of CN1  $\rightarrow$  CN2  $\rightarrow$  CN4 and F2  $\rightarrow$  F1  $\rightarrow$  F4  $\rightarrow$  F6.
4. In the case of PCH-based LCs (CN1, F4), SAS decreases drastically by replacing a cyano group with fluorine.
5. In cyano-LCs, SAS of a PCH-based LC (CN1) is about four times larger than that of a cyanobiphenyl-based LC (CN4).
6. By comparing CN4 with CN5 or F1 with F7, it can be seen that LCs with a high tendency to form dimers have large SAS values.

The tilt angle of the easy axis is controlled by the length and density of the lateral chain fragments of the diamine components in the PI alignment layer. In trying to understand the above trends it is helpful to think of the LC molecules as being immersed in the alignment film and not just interacting with the top layer of the film. Hence the interaction between the LC molecules and the polymer chains inside the alignment film must be taken into account in the study of the anchoring energy. We now try to rationalise the observed trends concerning the changes in SAS values with the LC molecular structure.

Regarding 1 above, the increase in SAS on the introduction of an ethylenic linkage may be due to an increase of the LC molecular flexibility and an increase in steric hindrance between the LC molecules and polymer chains. The increase in electronic density in the molecular skeleton of the LC (as in 2 and 3) may lead to increased unfavourable interaction with the polar parts of the PI chains and hence to small SAS values.

Regarding 4, the decrease in surface energy on replacing the cyano group by a fluorine is presumably caused by a reduced polar interaction with the polymer molecules. The presence of the lateral fluorine may be a contributing factor. The origins of the large differences observed in 5 are not clear and require further future investigations.

The formation of dimers, as thought most likely for 6 above, may make the LC molecules more difficult to move away from the surface leading thus to increased SAS values. To confirm this, 67.9wt.% of CN1 and 32.1wt.% of F1 were mixed and SAS was measured. The  $\Delta\epsilon$ ,  $k_{11}$ ,  $k_{22}$ , and  $k_{33}$  were 9.3, 8.0[pN], 6.7[pN], and 15.9[pN], respectively. The obtained SAS value was  $5.0 \times 10^{-4} \text{ [J/m}^2\text{]}$  which was half of CN1's SAS. This implies the dissociation of CN1 dimers by the addition of F1 molecules.

The relation between the tilt angle of the easy axis and SAS at 25°C for the cyano- and fluorinated liquid crystals is shown in Figure 4.

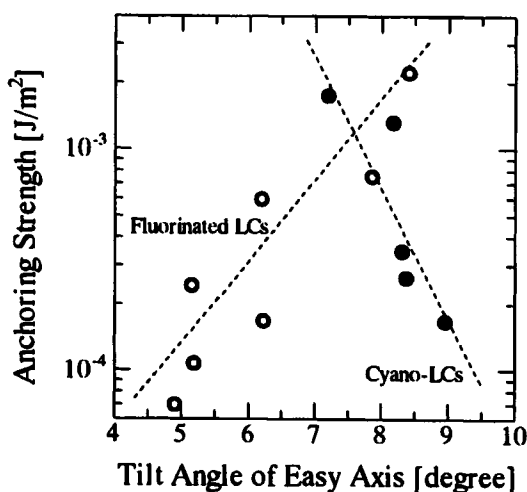


FIGURE 4 Relationship between surface anchoring strength and tilt angle at 25°C

The tilt angle for the cyano-LCs decreases as the value of SAS increases. On the other hand, for the fluorinated liquid crystals the reverse trend is observed: the tilt angle increases as the value of SAS increases. In general reports that appeared in the literature only speak of the tilt angle decreasing as the value of SAS increases<sup>[10]</sup>, here in the fluorinated LCs we observe the reverse.

The differences in the skeleton of the LC molecules used could be considered as one of the factors. Other factors involved in determining the SAS value could be the electronic interaction between the LC molecules and the alignment polymer, steric hindrance, order parameters and so on. To understand more about the mechanism of surface anchoring, molecular

model simulations as well as further systematic experimental investigations are required and planned.

## CONCLUSION

The surface anchoring strength (SAS) and the tilt angle on a polyimide alignment film surface were investigated for various cyano-LCs and fluorinated LCs with different molecular skeletons. Depending on the molecular structure of the LC, the value of SAS was found to vary over the range  $10^{-4}$  to  $10^{-3}$  [J/m<sup>2</sup>]. It was also found that the relationship between the tilt angle and SAS vary in opposite directions for the cyano- and fluorinated liquid crystals.

In the analysis of SAS values, the steric restriction by the polymer chains of the movement of LC molecules inside the alignment film was considered an important factor which cannot be ignored.

To understand further the detailed relation between the SAS, the tilt angle and the various molecular structures of the liquid crystals and the alignment polymer more detailed experimental investigations and modeling of LC conformations are necessary.

## References

- [1] B. Jérôme, *Rep. Prog. Phys.* **54**, 391(1991).
- [2] P.G. de Gennes, *The Physics of Liquid Crystals* (Oxford University, London, 1974).
- [3] A. Rapini and M. Papoular, *J. Phys. (Paris) Colloq.* **30**, C4-54(1969).
- [4] L.M. Blinov and V.G. Chigrinov, *Electrooptic Effects in Liquid Crystal Materials* (Springer-Verlag, New York, 1994).
- [5] A. Sugimura and Z. Ou-Yang, *Phys. Rev. E*, **51**, 784(1995).
- [6] A. Sugimura, G.R. Luckhurst and Z. Ou-Yang, *Phys. Rev. E* **52**, 681(1995).
- [7] A. Sugimura, K. Matsumoto, Z. Ou-Yang and M. Iwamoto, *Phys. Rev. E* **54**, 5217 (1996).
- [8] A. Sugimura, T. Miyamoto, M. Tsuji and M. Kuze, *Appl. Phys. Lett.* **72**, 329 (1998).
- [9] K.R. Welford and J.R. Sambles, *Mol. Cryst. Liq. Cryst.* **147**, 25 (1987).
- [10] Y. Iimura and S. Kobayashi, *Soc. Inform. Display, Tech. Diges* **28**, 311 (1997).